Measurement of the hard-sphere equation of state using screened charged polystyrene colloids

M. A. Rutgers*
Department of Physics, Princeton University, Princeton, New Jersey 08544

J. H. Dunsmuir
Exxon Research and Engineering Company, Route 22 East, Annandale, New Jersey 08801

J.-Z. Xue†
Department of Physics, Princeton University, Princeton, New Jersey 08544
and Exxon Research and Engineering Company, Route 22 East, Annandale, New Jersey 08801

W. B. Russel
Department of Chemical Engineering, Princeton University, Princeton, New Jersey 08544

P. M. Chaikin
Department of Physics, Princeton University, Princeton, New Jersey 08544
and Exxon Research and Engineering Company, Route 22 East, Annandale, New Jersey 08801
(Received 12 July 1995)

Using a high-resolution digital x-ray camera we have accurately measured the density profiles of several sediments of highly screened polystyrene colloidal spheres suspended in water. From the integral of the profile with height we directly measured the osmotic pressure as a function of volume fraction. The results are in excellent agreement with calculations of the hard-sphere equation of state for both the crystalline and disordered states. These results demonstrate experimentally that particles with a hard-sphere force law indeed exhibit the liquid-solid phase transition at the predicted volume fractions.

The calculation of the ideal gas law was one of the early triumphs of statistical mechanics. The concepts of entropy and temperature were quantitatively justified as the microscopic theory of a gas of noninteracting point particles universally explained the equation of state measured for real gases. The next logical step toward a more realistic fluid is a gas of uniformly sized impenetrable spheres. This model system has received much attention,[1,2] since it is the simplest case for which a first-order phase transition between a disordered liquid and an ordered solid has been predicted. For a long time the issue has remained theoretical, since there were few instances where real systems in thermodynamic equilibrium could be taken as a good approximation to hard spheres. Even the theory has been surprisingly difficult, and no exact calculation for the entire phase diagram exists to date. Significant theoretical[3] and experimental[4–6] progress has been made in the last 20 years, first with the advent of precise molecular dynamics simulations and later through the development of submicrometer colloidal spheres, which closely approximate hard spheres and are small enough to equilibrate thermodynamically in short times. In this work we report an accurate measurement of the equation of state of several such colloidal suspensions which provide the best evidence to date that colloidal particles can behave as true hard spheres.

As is the case for the ideal gas, the free energy for hard spheres derives entirely from the entropy, and equilibrium is determined by maximizing the number of accessible states. The finite particle size of hard spheres introduces no additional energy terms since the energy is infinite if the particles overlap and zero otherwise. Unlike the ideal gas, the hard-sphere system has not one but two length scales; the average interparticle spacing, commonly recast as the number density n, and the particle radius a. These parameters can be combined to form the volume fraction $\phi = n(4/3)\pi a^3$, the only relevant dimensionless parameter of the system. The volume fraction can range from $\phi = 0$ to an upper limit where the

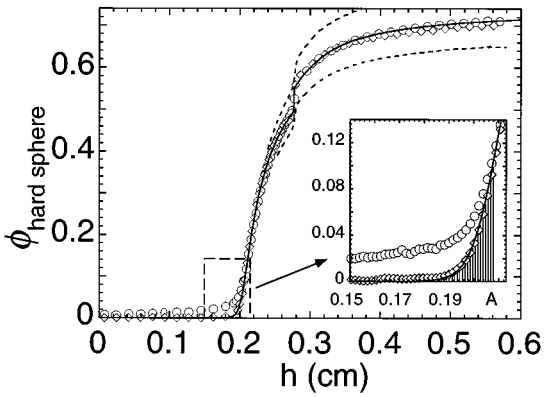

FIG. 1. Volume fraction profile for 0.720 μm diameter type *B* spheres. Main figure (90% of data points omitted for clarity): (—) calculated profile for true hard spheres, (○) raw data, (◇) digitally filtered data, (- - -) bounds set by systematic experimental error. Inset: **A** is the integration starting point; the shaded area is added to account for ignored particles.

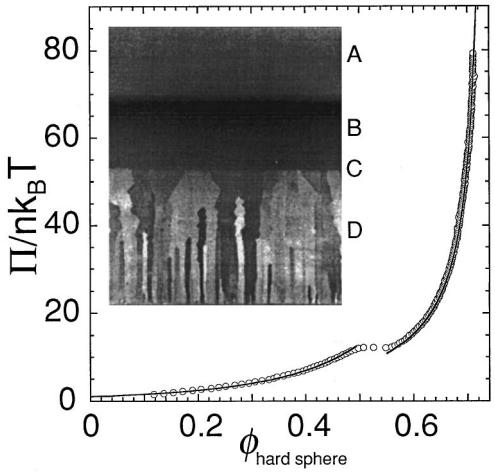

FIG. 2. Equation of state for 0.720 μm diameter type B spheres. (—) Calculated equation of state for true hard spheres. The inset shows a photograph ($\approx$1 cm) of the sample. (A) supernatant fluid, $\phi\approx 0$; (B) liquid phase, $0<\phi<0.494$; (C) sharp interface; (D) crystalline phase, $0.545<\phi<0.74$.

spheres are forced to touch and the pressure diverges. This can happen in two distinctly different ways: (1) formation of a randomly close packed Bernal[7] glass with a maximum volume fraction $\phi\approx 0.64$, (2) at some lower volume fraction the spheres may form neatly packed hexagonal planes, which can then be compressed to the absolute geometrical limit of $\phi=\pi/\sqrt{18}\approx 0.74$. Monte Carlo simulations[3] show that, in order to maximize the entropy of the system, a quasistatically compressed hard-sphere gas will never reach the glassy state, but undergo a first-order phase transition from a fluid-like state to a state with long range order. A coexistence between a fluid with $\phi=0.494$ and a solid with $\phi=0.545$ has been predicted. Thus the spheres actually give up long range positional freedom to relieve local overcrowding and maximize the entropy, which is the sole consideration of the system.

To date no exact calculation predicts this transition, but several useful expressions agree well with the Monte Carlo simulations. The full calculated equation of state can be summarized as

$$\Pi(\phi)=nk_BTZ(\phi), \tag{1}$$

where $Z(\phi)$, known as the compressibility factor, describes the deviation from the ideal gas law. For the fluid phase the Carnahan and Starling[8] result

$$Z(\phi)=\frac{1+\phi+\phi^2-\phi^3}{(1-\phi)^3} \tag{2}$$

provides an accurate semiempirical extension to solutions from the Percus Yevick equation. For the solid phase the expression

$$Z(\phi)=\frac{2.22}{0.74-\phi} \tag{3}$$

is a good approximation, though a more accurate but more complicated form was developed by Hall.[9]

A standard test for the hardness of real spheres has been to compare the equation of state to the calculations. Verification is especially important at high volume fractions where the characteristic length of the interparticle potential becomes comparable to the mean separation between particle surfaces. The equation of state for colloids with nearly hard potentials, such as sterically stabilized silica[5] and $PMMA$,[6] has mostly been measured by extrapolating the static structure factor to zero wave vector, where this quantity is proportional to the compressibility. This method has been implemented through both neutron[10] and light scattering,[11,12] but has not been extended beyond $\phi\approx 0.3$ because the structure factor becomes increasingly difficult to extrapolate to zero wave vector. Genz *et al.*[13] on the other hand have calculated that the equation of state is relatively insensitive to sphere hardness for $\phi<0.4$ and have also shown other methods, such as measuring the position of the principal maximum in the structure function, to be unreliable.

Another method of measuring the equation of state was introduced as early as 1910 when Jean Perrin, while measuring aspects of Brownian motion, noted that one could measure the osmotic pressure of pollen particles by observing their sediments.[14] The density profile in an equilibrium sediment is determined by the balance between gravitational forces and the osmotic pressure gradient. The osmotic pressure Π at any height z_0 must support the sum of the weight of the overlying particles, or

$$\Pi(z_0)=\int_{z_0}^{\infty} n(z)\Delta m_p g\,dz, \tag{4}$$

where g is the gravitational acceleration, n is the particle number density, and Δm_p is the buoyant particle mass. If the particle column is high enough, the bottom will be nearly close packed, and measuring a single density profile will yield the equation of state for the entire allowable range of volume fractions. This also eliminates the need for a separate sample for each volume fraction.

For this simple and elegant measurement to succeed, the density profile must be measured accurately. Several attempts have been made, notably by Hachisu and Takano,[15] more recently by Piazza *et al.*[16] The former experiment did not achieve sufficient resolution to resolve the details of the equation of state, whereas the latter reported discrepancies which may imply that the particles used were not good hard spheres. We have opted to measure density profiles using x-ray densitometry with a two-dimensional (2D) area detector, as opposed to the scanning beam method of Davis *et al.*[17] X-ray densitometry is more accurate and flexible than previous methods since it (1) is independent of the material optical properties, (2) averages over the full volume of the sample, ensuring good signal to noise, (3) is nondestructive, (4) probes at all heights simultaneously, eliminating any noise due to instrument drift.

For the experiments we suspended polystyrene spheres in water. Electrostatic repulsion between the particles keeps the suspension stable and the strength of the interaction can be screened with an added electrolyte. To maintain a nearly hard polystyrene sphere the repulsion should just overcome the van der Waals attraction between spheres. We estimated the interactions from various simplified interparticle potentials[18] and chose electrolyte concentrations of $3mM$ and $6mM$ HCl (Fig. 3, inset). As a measure of the potential steepness, the width over which it rises from $0.5k_BT$ to $5k_BT$ above the

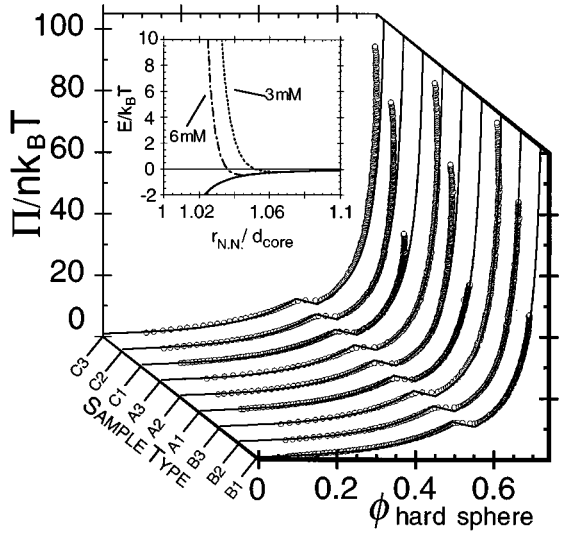

FIG. 3. Equation of state for the nine different samples of three effective particle diameters d_{HS} and three suspension preparations, described in Table I. Solid lines denote theory, (○) denote data. Inset: Typical calculated interparticle potential energy vs normalized particle separation $r_{\mathrm{NN}}/d_{\mathrm{core}}$. Solid line: van der Waals attraction. Dotted lines: sum of van der Waals and electrostatic repulsion, marked with added electrolyte concentrations.

minimum value is typically less than a few percent of the sphere core diameter d_{core}. This rise in the potential is centered about an effective hard-sphere diameter d_{HS} a few percent larger than d_{core}. Since the surface potential of the particles is generally not well known we leave d_{HS} as our only adjustable parameter. Calculations also showed that for the higher acid concentration the potential fails to significantly screen the attraction, which should have a detrimental effect on hard-sphere behavior.

At our disposal was a precision digital camera, developed for x-ray microtomography[19] using Molybdenum $K\alpha$ x rays (17.4 keV) source. The absorption coefficients are 1.21 cm^{-1} for water and 0.63 cm^{-1} for polystyrene, giving ample contrast at low concentrations and comparable photon count rates for all concentrations. The x rays emanated from a 0.4 mm$\times$0.8 mm rectangular area, traveled through 65 cm of air and through the 1 cm thick sample, and were then converted to visible photons by a 1 mm thick scintillator crystal which sat directly behind the sample. With a lens the light was imaged onto a cooled CCD chip (1024$\times$ 640 pixels). In our case we mapped a sample of 1 cm^2 onto about 500 pixels squared, limiting the spatial resolution to 20 μm. Due to the divergence of the incoming beam, the points furthest removed from the optical axis experienced a blurring of 2–3 pixels.

Polystyrene spheres with 0.596, 0.720, and 0.806 μm core diameters with standard deviations of 1.3%, 0.7%, and 1.4%, respectively, were purchased from Duke Scientific (Palo Alto, CA). For each sphere size three different sample treatments were selected. For the type *A* treatment we added diluted HCl directly to the stock solution to bring the final concentration to 6 mM. The last two types were first tumbled for 24 h in Fischer Rexyn 300 ion exchange resin, to remove any unwanted ions and surfactants, before the HCl was added. The final HCl concentrations were 3 mM for type *B* and 6 mM for type *C*. All samples (nine in total) had initial volume fractions of 0.1. Standard methacrylate spectrophotometry cuvettes (1 cm $\times$ 1 cm $\times$ 4 cm) were each filled with 2 cc of suspension and sealed. These nine samples were chosen to explore different particle sizes, stock suspension quality, and effect of the thickness of the particle double layer on their equation of state. The samples were left to sediment near the x-ray beam and were shielded from the $\approx$1 °C temperature fluctuations of the room.

After 3 months the samples had completely settled into a layer of crystallites (visible due to Bragg scattering of light) covered by a noniridescent fluid phase, which gradually gave way to the clear supernatant water (Fig. 2 inset). Five minute exposures were taken of each sample ($I_{T,S}$), accompanied by exposures of a cuvette filled with water ($I_{T,W}$), and a CCD dark current count D. The transmitted intensity I_T decays exponentially with distance, $I_T = I_0 e^{-\mu x}$, where μ is the attenuation coefficient, x is distance, and I_0 is the incident intensity. This relation is satisfied for each pixel in the image. We accounted for the nonuniform intensity profile of the incident beam, possible thickness variations in the scintillator, and the dark count of the CCD chip, as follows:

$$\frac{I_{T,S}-D}{I_{T,W}-D}=\frac{I_0 e^{-[\mu_w \delta(1-\phi)+\mu_p \delta\phi]}}{I_0 e^{-\delta\mu_w}}=e^{\delta[\phi(\mu_w-\mu_p)]}, \quad (5)$$

where δ is the sample thickness, and μ_w and μ_p are x-ray attenuation coefficients for, respectively, the water and the particles. The log of this ratio is now directly proportional to the particle volume fraction. For each size of spheres three reference samples of 5%, 10%, and 15% volume fraction were prepared, but were not allowed to sediment. From their images we measured linear x-ray attenuation coefficients as a function of particle core volume fraction.

Figure 1 shows a typical volume fraction profile for the type *B* particles (0.720 μm core diameter), taking the density of water as 0.997 gr/cc and the density of the spheres as 1.05 gr/cc. For an effective particle diameter of $d_{\mathrm{HS}}=0.730\pm0.026$ μm the data and theory are in excellent agreement, including the jump in volume fraction between the coexisting liquid and solid phases. The uncertainty in d_{HS} is purely a reflection of the systematic measurement errors in the liquid density, particle density, volume fraction calibration, x-ray intensity stability, and spatial CCD calibration. For a rms uncertainty of all the system parameters a fit of equal quality to Fig. 1 is achieved with the quoted error in d_{HS}, because the data are linearly related to all these parameters. The two bounding curves in Fig. 1 show the linear scaling of the data with the rms total systematic error, which should be improved by a factor of 5 when we carefully monitor the x-ray generator output in future experiments. Additional measurements made 6 months later were indistinguishable and proved the samples had indeed equilibrated.

From the ideal gas law we expect the volume fraction to decrease exponentially with height at low volume fraction, but instead we measured a very long tail at the top of the bed, which was not visible in the sample with the naked eye. The camera lens proved to be at fault, e.g., an optical image of black tape on a translucent white background, illuminated from behind, showed the same long tail. Hence we used such

TABLE I. Effective hard-sphere diameters (in μm) for best fits of data in Fig. 3. Errors denote systematic uncertainties. Types *A* and *C*: 6 mM HCl, type *B*, 3 mM HCl. See text for further type descriptions.

d_{core}	Type *A*	Type *B*	Type *C*
0.596(1)	0.648±3.1%	0.673±3.0%	0.654±3.1%
0.720(2)	0.761±3.0%	0.793±3.0%	0.772±3.2%
0.806(3)	0.854±3.0%	0.877±3.1%	0.859±3.1%

sharp edge images to find the line spread function of the optical system and the image restoration technique of partial inverse digital filtering (Ref. 20, pp. 212–217) to deconvolve our data. The filter successfully removed the tail, while changing only slightly the rest of the profile (Fig. 1). Use of superior lenses should eliminate the problem and avoid the use of image restoration techniques which are notorious for introducing noise.

The integral of the volume fraction profile is shown in Fig. 2, along with the calculated equation of state. The data, normalized by nk_BT in the figures, cover an absolute pressure range between 0 and 10 dyn/cm^2 with a resolution better than 0.1 dyn/cm^2. Since the digital filtering technique introduces noise at the higher volume fractions, where the data are most interesting, we opted not to use it for the integration of Eq. (4). Instead we ignored the low volume fraction tail by starting the integration at point *A* in Fig. 1 (inset). We add the shaded area to the integral, as calculated with Eqs. (1) and (2) (to make up for any particles ignored along with the tail) and see beautiful agreement with the calculations, for the large range of $0.12<\phi<0.70$.

Figure 3 gives an overview of the data from the different samples, and Table I lists the effective particle diameters d_{HS} which are within the scope of our calculations for a reasonable range of particle surface charge densities ($10^{-2}<\sigma<10^{-4}e^-/$ Å^2). We did not observe the anomalous 30–50 % apparent reduction of the effect of gravity on the particles measures by Piazza *et al.*,[16] who accordingly rescaled their particle mass to achieve optimal agreement with theory.

For the type *B* preparation the data agree perfectly with theory, but for the others the pressure reads consistently high at high volume fractions, and even tends to ''double back.'' One possibility is a large number of crystal defects toward the bottom of the samples, which reduces the density below that expected for hard spheres. This is consistent with the data for types *A* and *C* which do not comply at volume fractions which correspond to the bottoms of the samples. This means that the more tightly screened particles somehow did not crystallize fully before the overburden of sedimenting material locked in some level of disorder. Our calculations of the interparticle potentials suggest that a slight attraction for the more tightly screened particles affects the crystallization rate, though it is not clear why this only happened early in the sedimentation process. There is other evidence in the literature that sedimenting silica hard spheres usually do not form good crystals at the very bottom of the container, but start out with an amorphous layer, followed by iridescent crystals.[21]

The x-ray densitometry technique outlined here is of considerable value for measuring colloidal interactions. It is nondestructive, is not sensitive to the optical properties of the materials, and can have very high spatial resolution. The method is not only effective for volume fractions up to close packing, but measures particle interactions for large ranges of concentration in a single measurement, with a single sample. Our first results using this technique are in excellent agreement with the calculations for the hard-sphere equation of state and show that tightly screened polystyrene spheres closely approximate real hard spheres. Moreover they demonstrate that our particles exhibit the liquid-crystalline solid transition at the volume fraction predicted theoretically.

This research was supported in part by NASA under Grant No. NAG3-1158.

*Author to whom correspondence should be addressed. Current address: Dept. of Physics, University of Pittsburgh, Pittsburgh, PA 15260.

†Current address: Displaytech Inc., 2200 Central Ave., Boulder, CO 80301.

[1] W. W. Wood and J. D. Jacobsen, J. Chem. Phys. **27**, 1207 (1957).
[2] B. J. Alder and T. E. Wainwright, J. Chem. Phys. **27**, 1208 (1957).
[3] B. J. Alder, W. G. Hoover, and D. A. Young, J. Chem. Phys **49**, 3688 (1968).
[4] M. E. Woods *et al.*, J. Paint Technol. **40**, 541 (1968).
[5] A. K. van Helden, J. W. Jansen, and A. Vrij, J. Colloid Interface Sci. **26**, 62 (1981).
[6] L. Antl *et al.*, Colloids Surf. **17**, 67 (1986).
[7] J. Bernal, Proc. R. Soc. A **280**, 299 (1964).
[8] N. F. Carnahan and K. E. Starling, J. Chem. Phys **51**, 635 (1969).
[9] K. R. Hall, J. Chem. Phys. **57**, 2252 (1972).
[10] I. Markovic, R. H. Ottewil, S. M. Underwood, and T. F. Tadros, Langmuir **2**, 625 (1986).
[11] A. Vrij *et al.*, Faraday Discuss. Chem. Soc. **76**, 19 (1983).
[12] I. Livsey and R. H. Ottewil, Colloid Polym. Sci. **267**, 421 (1989).
[13] U. Genz, B. D'Aguanno, J. Mewis, and R. Klein, Langmuir **10**, 2206 (1994).
[14] J. Perrin, J. Phys. (Paris) **9**, 5 (1910).
[15] S. Hachisu and K. Takano, Adv. Coll. Int. Sci. **16**, 233 (1982).
[16] R. Piazza, T. Bellini, and V. Degiorgio, Phys. Rev. Lett **71**, 4267 (1993).
[17] K. E. Davis, W. B. Russel, and W. J. Glantsching, J. Chem. Soc. Faraday Trans. **87**, 411 (1991).
[18] W. B. Russel, D. A. Saville, and W. R. Schowalter, *Colloidal Dispersions* (Cambridge University Press, Cambridge, 1991).
[19] B. Flannery, H. Deckman, W. Roberge, and K. D'Amico, Science **237**, 1439 (1987).
[20] J. C. Russ, *The Image Processing Handbook*, 1st ed. (CRC, Boca Raton, 1992).
[21] K. E. Davis, W. B. Russel, and W. J. Glantsching, Science **245**, 507 (1989).